Fabrication of a Stretchable Solid-State Micro-Supercapacitor Array

Daeil Kim,[†,⊥] Gunchul Shin,[†,⊥] Yu Jin Kang,[‡] Woong Kim,[‡] and Jeong Sook Ha[†,§,*]

[†]Department of Chemical and Biological Engineering, Korea University, Seoul 136-701, Republic of Korea, [‡]Department of Materials Science and Engineering, Korea University, Seoul 136-713, Republic of Korea, and [§]KU-KIST Graduate School of Converging Science and Technology, Korea University, Seoul 136-701, Republic of Korea. [⊥]These authors have equally contributed in this paper.

ABSTRACT We fabricated a stretchable micro-supercapacitor array with planar SWCNT electrodes and an ionic liquid-based triblock copolymer electrolyte. The mechanical stability of the entire supercapacitor array upon stretching was obtained by adopting strategic design concepts. First, the narrow and long serpentine metallic interconnections were encapsulated with polyimide thin film to ensure that they were within the mechanical neutral plane. Second, an array of two-dimensional planar micro-supercapacitor with SWCNT electrodes and an ion-gel-type electrolyte was made to achieve all-solid-state energy storage devices. The formed micro-supercapacitor array showed excellent performances which were stable over stretching up to 30% without any noticeable degradation. This work shows the strong potential of a stretchable micro-supercapacitor array in applications such as wearable computers, power dressing, electronic newspapers, paper-like mobile phones, and other easily collapsible gadgets.

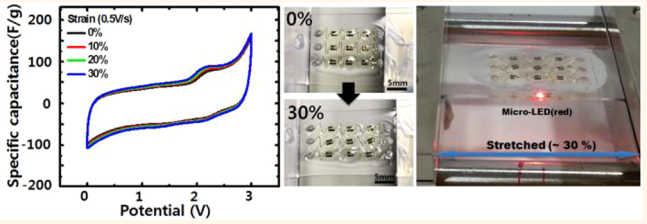

KEYWORDS: micro-supercapacitor · SWCNT electrode · stretchable · ion-gel electrolyte

Due to the increasing demand for personal and portable electronics applicable to future wearable and bioimplantable systems, it has become increasingly more important to fabricate stretchable and curvilinear electronic devices instead of conventional rigid devices. Since the clothes we wear and the human body, including the skin and organs, have nonflat surfaces, the contact between them and the conventional rigid and flat electronic devices is nonconformal, limiting the performance and efficiency to be directly applied to wearable and implantable systems. Recently, many researchers have reported on the fabrication of various types of stretchable devices such as stretchable logic devices,[1−3] organic[4]/inorganic[5,6] LEDs, photodetectors,[7−11] and bioimplantable devices.[12−16] A strain-compensated structure is used in these devices for stable operation over the deformation such as stretching, contracting, or twisting. However, operation of most of the stretchable devices required the use of external power connected *via* physical wiring since no energy storage device was embedded. Therefore, it is necessary to have stretchable energy storage devices integrated into the stretchable electronic devices for their application to wearable or bioimplanted systems without an external power supply.

Recently, extensive reports have been presented on the fabrication of flexible and stretchable powering systems on paper or elastomers including photovoltaics,[17] RF power transmission,[18] secondary batteries,[18−22] and supercapacitors.[22−30] Among these, supercapacitors have many advantages such as high power density, safety, long durability, and relatively simple design. However, up to now, the elastic deformation of the stretchable supercapacitors fabricated has depended on the prestrain applied to the substrate prior to the fabrication of the supercapacitors and on the stretchability of the component materials.[28] It is therefore difficult to integrate the supercapacitors into a stretchable electronic circuit. So, two-dimensional (2D) planar micro-supercapacitors would be a possible solution for integration into stretchable electronic circuits since they are relatively easy to design and pattern with micrometer-sized channel length. Furthermore, a 2D planar structure would reduce the ionic diffusion pathway, thus producing a high power density of micro-supercapacitors.[29]

* Address correspondence to jeongsha@korea.ac.kr.

Received for review June 18, 2013 and accepted August 16, 2013.

Published online August 16, 2013
10.1021/nn403068d

Here, we report the fabrication of a stretchable micro-supercapacitor array based on all-solid-state materials. To achieve the mechanical stability over deformation, we adopted two strategic design concepts of long and narrow serpentine interconnections in a mechanical neutral plane and a planar micro-supercapacitor array. In particular, a 2D planar supercapacitor array was fabricated by patterning of spray-coated SWCNTs as electrodes and by using an ionic-liquid-based triblock copolymer electrolyte. The micro-supercapacitior array showed a capacitance of ~100 μF at a scan rate of 0.5 V/s. Device performance was stable over stretching up to 30%.

RESULTS AND DISCUSSION

Figure 1 schematically shows the fabrication process of a stretchable micro-supercapacitor array on an elastomeric PDMS substrate as follows: spin-coating of 400 nm thick polyimide film on SiO_2/Si substrate, deposition of patterned electrodes and interconnections of Ti/Au (5 nm/50 nm) by e-beam evaporation, spray-coating of SWCNT electrodes, spin-coating of 400 nm thick PI film, detachment of entire structure *via* tape transfer method and subsequent attachment to PDMS substrate, drop-casting of ion-gel electrolyte, and final encapsulation with 0.5 mm thick PDMS film. A detailed description of the fabrication is given in the Methods section. Metallic interconnections of Ti/Au were designed to be narrow and in a long serpentine shape for better deformational stability and encapsulated by thin PI film to ensure they are within the mechanical neutral plane.[8]

The cross-sectional drawing given in the bottom of Figure 1 clearly shows the fabricated planar micro-supercapacitor. As marked by the two arrows, the charge−discharge mechanism is quite simple in such a planar supercapacitor.[29,30] When a DC bias is applied across the electrodes of the supercapacitor, positively charged ions in the electrolyte move toward the negatively biased electrode and are adsorbed to form an electric double layer while the negatively charged ions move and are adsorbed on the positively charged electrode. In this planar structure without a polymer separator between electrodes, both ions in the ion-gel electrolyte move without resistance. Discharging proceeds by releasing electrons upon connection of the supercapacitor to a resistor.[29] Use of the 2D planar supercapacitor can have advantages. First, the electrodes can be patterned easily so as to be integrated on one chip by using a photolithography process. Second, the traveling distance of the ions in the electrolyte, a major factor to influence the performance in supercapacitors, can be well-controlled and shortened *via* eliminating the necessity of a separator and controlling the length between electrodes.[29]

As shown in Figure 2a, a 3 × 3 supercapacitor array connected with serpentine interconnections and six measuring electrodes was fabricated on a SiO_2/Si substrate. The 3 × 3 supercapacitor array was designed to be in parallel connection to produce total capacitance 9 times that of each supercapacitor (Supporting Information Figure S1). The complete device was transferred onto a PDMS substrate *via* the tape transfer method, a key step for the fabrication of a stretchable

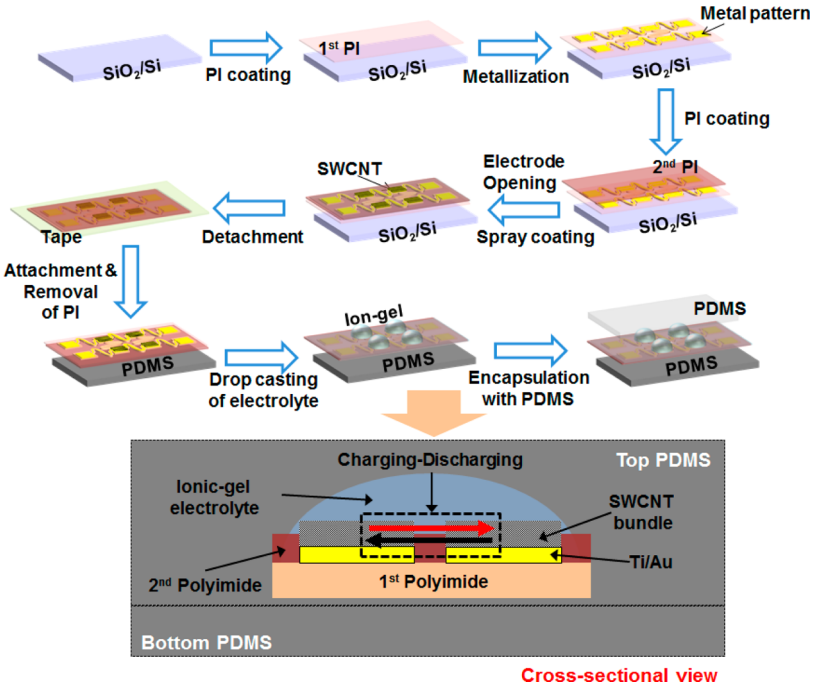

Figure 1. Schematics of fabricating a stretchable micro-supercapacitor array on a PDMS substrate (top) and a cross-sectional view of a micro-supercapacitor (bottom).

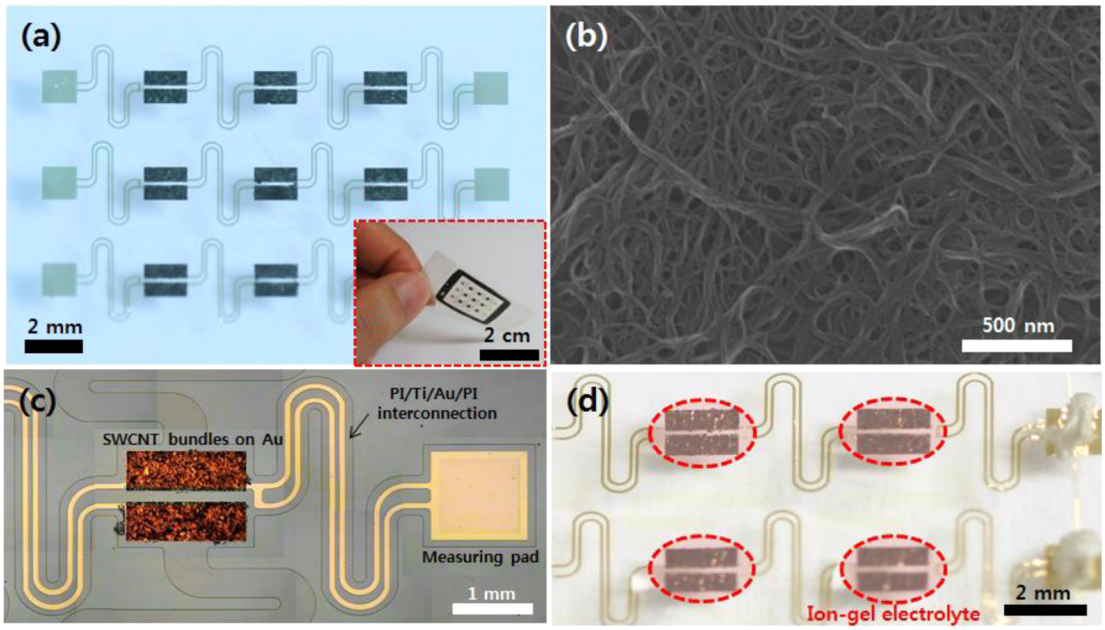

Figure 2. (a) Photograph of a stretchable 2D planar micro-supercapacitor array on a PDMS substrate without electrolyte. Inset image shows the tape-transferred micro-supercapacitor array. (b) SEM image of the SWCNT-COOH bundles on the Ti/Au current collector electrode. (c) Magnified optical microscope image of an individual micro-supercapacitor with serpentine interconnections. (d) Photograph of the 2D planar stretchable all-solid-state supercapacitors with ion-gel electrolyte.

supercapacitor array (inset of Figure 2a). Using the tape transfer method, neither the sacrificial layer nor chemical etching was carried out, which can be detrimental to the device performance.[3] Instead, the difference in the interfacial force between the PI film and SiO_2/Si substrate and that between PI film and the tape were used for the transfer process; the latter was larger than the former. Moreover, the PI film had sufficient robustness to prevent being torn when the entire film is detached from the SiO_2/Si substrate using the tape. As a result, the entire device array, including the electrodes, could be successfully transferred onto an elastomeric PDMS substrate.

Figure 2b shows the FESEM image of SWCNTs on a current-collecting electrode. The spray-coated SWCNT bundles with a pore diameter distribution of 10−100 nm are randomly deposited and entangled on a Ti/Au current collector. An optical microscope image of a stretchable supercapacitor with serpentine interconnections taken after being transferred onto a PDMS substrate and subsequent reactive ion etching (RIE) is shown in Figure 2c. Since the largest strain is applied to the joint between the SWCNT electrode and the interconnection upon stretching of the entire device, the rounding of the interconnection at the joints was designed as shown in the image.[31] The final stretchable supercapacitor array based on SWCNT electrode/ion-gel electrolyte, [EMIM][NTf_2], is shown in Figure 2d. Owing to the immiscibility of different repeating units of the block copolymer (*i.e.*, PS and PMMA), segregated nanostructures can be formed in the ion-gel electrolyte *via* a self-assembly process.[32−34] Here, the ionic liquid of the imidazolium family was selected due to its high capacitance and fast polarization response.[33,35,36] The ionic liquids separated into cation ($[EMIM]^+$) and anion ($[NTf_2]^-$) can be held in the nanoscale space surrounded by PMMA blocks, which are miscible with ionic liquids, whereas the PS blocks are not.[32−34]

Figure 3a shows the CV curves obtained from the 3 × 3 array of micro-supercapacitors. The CV curves of the supercapacitor were found to be rectangular in shape at scan rates between 0.5 and 4 V/s, indicating a highly stable performance of the fabricated micro-supercapacitors under a high potential of 3 V. In each planar micro-supercapacitor, two SWCNT electrodes of 0.5 mm × 1.5 mm are separated by 150 μm. The total mass of the SWCNT electrodes in the 3 × 3 supercapacitor array was calculated using the ratio of electrode area and the total area of the supercapacitor. The total deposited and electrode areas were 9 mm × 15 mm (135 mm^2) and 13.5 mm^2, respectively. In this work, the total amount of SWCNTs deposited onto the electrodes was estimated to be 2 μg. Capacitance of the supercapacitor was approximately 100 μF. Specific electrode capacitances (C_{sp}) were 55.3 and 34.2 F/g at scan rates of 0.5 and 4 V/s, respectively. The C_{sp} was calculated using the equation of $C_{sp} = (2 \times \oint I dV)/(M \times \Delta V \times S)$, where I is the measured current, M is the CNT mass of total electrode, ΔV is the operation voltage window, and S is scan rate.[25]

Figure 3b shows the charge−discharge curves at a constant current density of 25 A/g, and these were close to a triangular shape, confirming the high Coulombic efficiency, excellent reversibility, and good charge

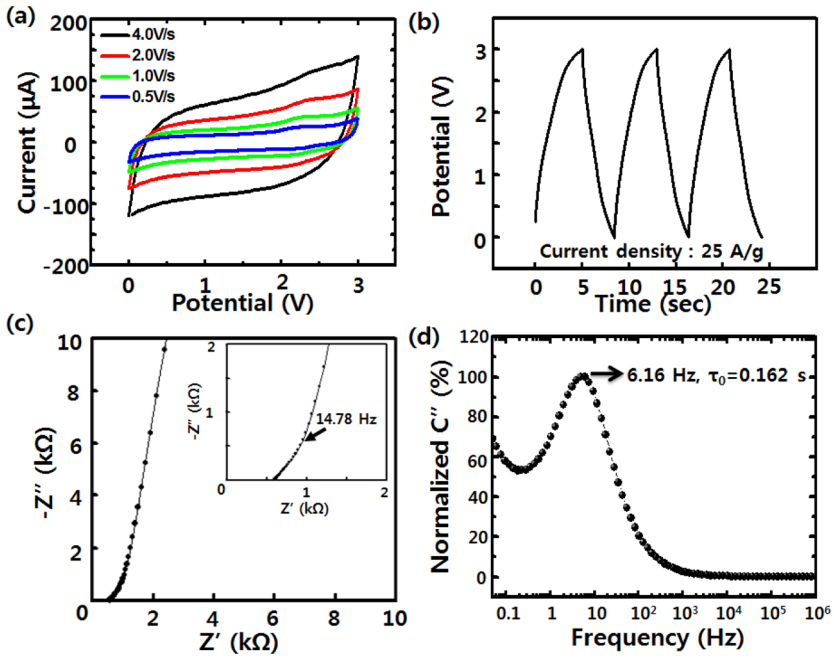

Figure 3. (a) CV curve, (b) galvanostatic charge−discharge curves, and (c) Nyquist plot of a spray-coated SWCNT-COOH electrode in an ion-gel electrolyte. A knee frequency of 14.78 Hz is indicated in the inset. (d) Normalized *C″* *versus* frequency. The extremely low τ_0 value of 0.162 s was extracted.

propagation across the two electrodes. Nyquist plots consistently exhibited excellent capacitive behavior, as indicated by the near vertical line over the low-frequency ranges (Figure 3c). A knee frequency of 14.78 Hz was observed, which is the maximum frequency at which capacitive behavior is dominant (inset of Figure 3c). Equivalent series resistance (ESR) estimated from the intercept of the curve on the *x*-axis was about 520 Ω at 75 kHz. Here, it is noted that a rapid frequency response of the stretchable supercapacitor was confirmed by a short relaxation time constant (τ_0); τ_0 is the reciprocal of the frequency (f_o) at the peak in the normalized capacitance (C'') versus frequency plot (Figure 3d); τ_0 is the transition point of the electrochemical capacitor from capacitive to resistive behavior and corresponds to the point of maximum energy dissipation. Thus, the short relaxation time indicates the rapid frequency response of the supercapacitor. In this work, τ_0 is estimated to be 0.162 s.[27,37]

Device performance was measured while stretching the entire device up to 30%. Figure 4a shows photographs of the supercapacitor array taken before and after stretching (top) and the CV curves (bottom). No noticeable damage or defects were observed in the entire device, including the operating SWCNT electrodes and interconnections after stretching by 30%. Photographs taken continuously while stretching from 0 to 30% are shown in Figure S2. Furthermore, the serpentine interconnections were stretched and deformed smoothly. CV curves were obtained with variation of the extent of stretching in two different ways: measurements with increasing (top indicated by ①) and decreasing (bottom indicated by ②) the strain as shown in Figure 4a. Upon increasing the strain from 0 to 30%, CV curves obtained at a scan rate of 0.5 V/s seem to show a slight decrease (①). A slight decrease of capacitance also seems to be shown with a subsequent decrease of strain from 30 to 0% (②). Since both processes ① and ② showed the slight decrease of the capacitance, we consider that such degradation was not simply due to mechanical deformation. There might be two possible causes of such degradation of stretchable supercapacitors: (1) deterioration of chemical properties of the supercapacitor and (2) deterioration of mechanical properties due to strain upon stretching.

It was reported that [EMIM][NTf_2] ionic liquid used for making ion-gel electrolyte in this experiment showed the decrease in the mobility by adsorption of water molecules in air.[38] Therefore, experiment using ionic liquid should be performed in vacuum or ambient N_2 to maintain the intrinsic capacitor performance. However, for the practical application of stretchable supercapacitors in ambient air, we encapsulated the whole device arrays with PDMS film to obtain the stretchability. PDMS, which has high water permeability, is not the best candidate for passivating the ionic-gel electrolyte from water adsorption but is almost best for the stretchable devices.[39] So, we consider there might be a slight degradation of the capacitance due to poor passivation by PDMS encapsulation, not protecting the deterioration of ionic-gel electrolyte under humid environment. For the practical application of stretchable supercapacitors in ambient air,

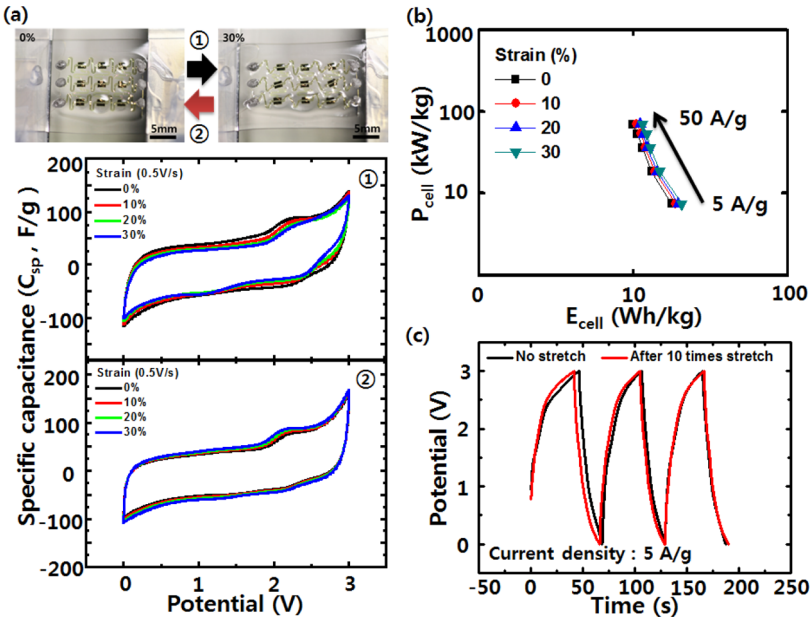

Figure 4. (a) Photographs of the entire device of the 3 × 3 micro-supercapacitor array before (top left) and after application of strain of 30% (top right). CV curves of ① were obtained while increasing the strain from 0 to 30%, and those of ② were obtained while decreasing the strain from 30 to 0%. (b) Ragone plots (power density *vs* energy density) were taken at various scan rates from 5 to 50 A/g under strain application from 0 to 30%. (c) Variation of galvanostatic charge/discharge curves at 5 A/g upon 10 times repetition of 30% stretching.

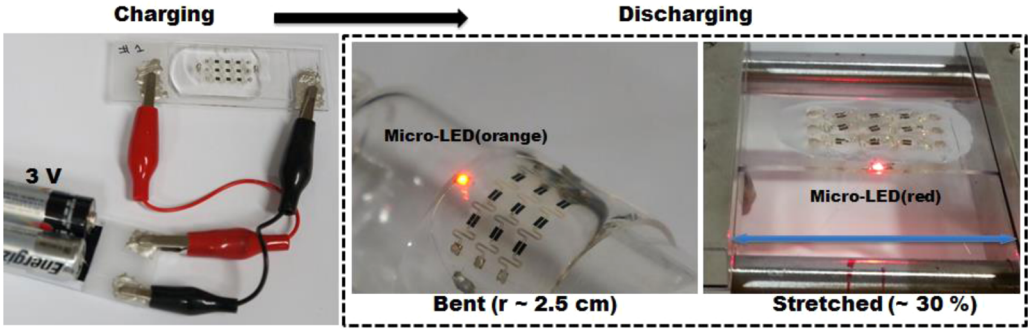

Figure 5. Photographs showing the charging state at 3 V (left) and discharging state lighting μ-LEDs under bent (center) and 30% stretched state (right).

other materials with better water-passivating properties and stretchability should be developed.

However, we cannot exclude the possible degradation of the supercapacitor upon repeated stretching and releasing the whole devices since the contact between the micro-supercapacitor and the Ti/Au interconnection would be deteriorated. Even though we successfully showed the mechanical stability of SnO_2 NW FETs upon stretching up to 30% with the similar design in our previous work,[40] the present design might not be optimized for the stretchable supercapacitor arrays; (1) the size of the active device, micro-supercapacitor, is ~150 times larger than the SnO_2 NW FET, so that larger strain is expected at the contact area; (2) since the ion-gel electrolyte-covered supercapacitor array was encapsulated with relatively thick PDMS film, larger strain is expected on the whole devices upon stretching compared to the air-exposed SnO_2 NW FETs. Since this work is the first approach to fabricate the stretchable supercapacitor arrays which can be integrated onto one-chip devices, there remains further improvement. In addition, excellent characteristics of our supercapacitor array are shown in a Ragone plot (Figure 4b). Curves taken from the supercapacitor array upon application of strain between 0 and 30% do not show a noticeable difference. The specific energy (E_{cell}) and power (P_{cell}) densities of a cell were estimated from the galvanostatic charge–discharge curves using the relationships of $C_{cell} = I/(M \times dV/dt)$, $E_{cell} = 0.5 \times C_{cell} \times V^2$, and $P_{cell} = E_{cell}/\Delta t$, where I is the applied current, and V and t are potential and time after IR drop, respectively. The maximum E_{cell} at a current density of 5 A/g was 20.7 Wh/kg at P_{cell} of 7.4 kW/kg. The maximum P_{cell}

value at a current density of 50 A/g was 70.5 kW/kg at E_{cell} value of 11.5 Wh/kg. Furthermore, the charge–discharge performance of the stretchable supercapacitor at a current density of 5 A/g was not nearly deteriorated even after 10 times repeated stretching by 30%, as shown in Figure 4c. These results confirm the mechanical stability of our stretchable micro-supercapacitor array.

The charge–discharge properties of the stretchable supercapacitor array are demonstrated by lighting a micro-light-emitting diode (μ-LED). The fabricated supercapacitor array was simply charged by a serially connected alkaline battery (3 V) for 60 s (Figure 5, left). After charging, the supercapacitor array was connected with a μ-LED. Both the orange and red colored μ-LEDs were lit at bent (bending radius = 2.5 cm, middle) and stretched (strain = 30%, right) states, respectively. No visible damage or defects in all the devices were observed. This also confirms the wide application of stretchable micro-supercapacitors in various future flexible and stretchable electronics.

CONCLUSION

In this study, we report on the fabrication of an all-solid-state stretchable supercapacitor array with high mechanical strength and good electrochemical performance under maximum strain of 30%. To ensure the mechanical stability upon deformation, we adopted two strategic design concepts of long and narrow serpentine interconnections in the mechanical neutral plane and the 2D planar micro-supercapacitor array. The supercapacitor composed of 2D planar SWCNT electrodes and ion-gel electrolyte showed excellent device performance, which was not deteriorated upon strain up to 30%. This solid-based stretchable supercapacitor demonstrates a high potential as an energy storage device for wearable computers, power dressing, electronic newspapers, paper-like mobile phones, and other easily collapsible gadgets.

METHODS

Preparation of Carboxylic-Acid-Functionalized SWCNT Solution for Spray-Coating. The SWCNTs (Carbon Nanotechnologies, Inc.) were functionalized by treatment with conventional acid. For acid treatment, 10 mg of SWCNTs was mixed with 30 mL of sulfuric acid (H_2SO_4, Sigma Aldrich, 99.999%), and the solution was stirred for 30 min. To form the carboxylic-acid-functionalized SWCNT (SWCNT-COOH) film, the solution was vacuum filtered using a polymer membrane filter (polytetrafluoroethylene (PTFE), pore size 0.5 μm, ADVANTEC MFS, Inc.). Five milliliters of SWCNT-COOH solution was poured into deionized water (DI water) on the membrane filter. The DI water was then continuously poured onto the SWCNT-COOH film during a filtration process to wash the SWCNT-COOH film. Subsequently, the SWCNT-COOH film on the membrane filter was dried in an oven at 70 °C for 2 h. The dried SWCNT-COOH film was dispersed in 500 mL of DI water with sonication for 1 h.

Fabrication of All-Solid-State Stretchable Supercapacitor Array. In order to obtain the uniformly coated PI film without delamination, we used diluted polyimide solution (polyamic acid solution (Aldrich)/PI thinner (1-methyl-2-pyrrolidinone/aromatic hydrocarbon solvents, Aldrich) = 4:1 by wt) that was mixed for 2 h by using Vortex Genie-2 (Scientific Industries, Inc.) and remained for 24 h to remove the bubble in diluted PI solution. Diluted polyimide solution was spin-coated onto the SiO_2/Si substrate in a two-step scheme at 500 rpm for 10 s and 4000 rpm for 60 s. After annealing the PI-coated substrate at 95 °C for 3 min and at 150 °C for 10 min in air, it was cured at 250 °C for 2 h under Ar. The uniformity of the 400 nm thick PI film was confirmed by taking the AFM images as shown in Figure S3. In particular, we do not apply severe mechanical disturbance such as ultrasonication since the spin-coated PI film was delaminated when we used ultrasonication for lift-off during the photolithography process. Instead, we used lift-off resist (LOR), which assisted the lift-off process by forming the undercut. The image of the undercut photoresist is shown in Figure S4. In addition, removal of the residual surface contaminants on the device substrate such as dust was done by a gentle blowing with N_2 gas.

To form the current collector, measurement pad, and interconnections, a photoresist film pattern was fabricated on the first PI film-coated substrate *via* a photolithography process. Here, two layers of photoresist film were deposited by spin-coating. The first photoresist, lift-off resist (K1 solution), was spin-coated in a two-step scheme at 500 rpm for 10 s and 2000 rpm for 30 s and then annealed at 170 °C for 1 min. The second photoresist (AZ5214, Microchemicals) was coated under the same condition used for LOR and then annealed at 110 °C for 1 min.

After e-beam evaporation of Ti (5 nm)/Au (50 nm) electrodes for a current collector, the diluted PI solution was spin-coated onto the substrate again to form a neutral mechanical plane for Ti/Au. Subsequently, the current-collecting electrode and measured electrode were opened *via* photolithography and RIE for 5 min (150 W DC power, 45 mTorr pressure, and 20 sccm O_2 flow). Then, functionalized SWCNT-COOH solution was spray-coated on the patterned current-collecting electrodes. During the spray-coating, the substrate was heated at 90 °C for evaporation of water. The weight of the deposited SWCNT-COOH electrodes was measured using a microbalance (OHAUS, Adventurer). During this process, we used the photolithography for patterned deposition of SWCNT bundles on the metal electrode (current collector parts) by spray-coating. As shown in the schematic illustration of Figure S4, SWCNTs were spray-coated on the patterned Ti/Au electrode where the LOR was used on top of the second PI film to form the undercut for easier lift-off after the SWCNT coating. After fabrication of the SWCNT-COOH electrodes, the photoresist was removed with acetone by a gentle lift-off process, and then the LOR was removed with developer (AZ300, Microchemicals) for 10 s (Figure S4). As a result, SWCNT patterns with clean edges which were not connected with each other could be obtained, as shown in the optical microscope images of Figure S4.

An opening pattern for removing the PI film was then made using photolithography with alignment. The prepared supercapacitor electrode pattern array on the SiO_2/Si substrate with the opening pattern was transferred onto the square-shaped PDMS substrate. The transfer was as follows: 5 cm long commercial plastic tape (3M) was prepared, and both ends (1 cm) were folded over to grab properly without tape adhesive. The center part of the tape, which has the same size as the active area of the supercapacitor array, was removed by blazer. After attaching the tape on the edge of the device not on the active area, it was gently detached from the SiO_2 substrate since the adhesion between the tape and the device layer is stronger than that between the device layer and SiO_2 substrate.[40] Double layer of PI film used here was sturdy enough to detach the whole film with device arrays, even though there was no tape in the center area. Detached device layers with tape were placed on the PDMS substrate. After etching of residual PI area using oxygen plasma etching (150 W DC power, 45 mTorr, and 20 sccm O_2 flow), the tape attached on the edges was removed only.

Active area of the device array remained on the PDMS substrate since there was no connection between the tape and device arrays. This tape transfer method was performed at room temperature in a dry environment without any chemicals. The transferred sample was rinsed carefully with acetone to remove the residual photoresist.

The ionic-liquid-based solid (gel) electrolyte was formed by adding 524 mg of the triblock copolymer (poly(styrene (PS)-*block*-methyl methacrylate (PMMA)-*block*-styrene, Polymer Source Inc., 10 wt %) in 3 mL of [EMIM][NTf_2](C-TRI). The number average molecular weights of each polymer were M_n(PS) = 5.8 kg/mol and M_n(PMMA) = 118 kg/mol. The mixture was dissolved in 20 mL of acetonitrile and magnetically stirred for 12 h in a nitrogen atmosphere using a Schlenk line. The acetonitrile was removed at 130 °C for 24 h using a vacuum line.[25] Ten microliters of solid electrolyte was drop-coated onto the top surface between the SWCNT electrodes of the individual micro-supercapacitor using a syringe. For encapsulation of the supercapacitor, the entire device was coated with PDMS solution and then cured at 70 °C for 1 h. To avoid the mixing of ion-gel with PDMS, cured thin PDMS (solid state and thickness ~500 nm) film was attached on the whole device array, and then the gel state PDMS was poured next.

Characterization of All-Solid-State Stretchable Supercapacitor. External strain was applied to the entire supercapacitor array using a homemade stretching stage. Under strain application between 0 and 30%, measurements of cyclic voltammetry, galvanostatic charge−discharge curve, and Nyquist plot were performed using an electrochemical analyzer (Ivium Technologies, Compact Stat). FESEM (S-4800, Hitachi) and photographic (Galaxy S III (Samsung) and Eos 7D (Canon)) and optical microscope (BX41M, Olympus) images were recorded. The charge−discharge performance of the micro-supercapacitor array was measured by connecting μ-LEDs. The specs of the μ-LEDs (ROHM comp. China) were 2.0 V, 20 mA, and 100 mcd (orange light) and 2.0 V, 20 mA, and 85 mcd (red light), respectively.

Conflict of Interest: The authors declare no competing financial interest.

Acknowledgment. This work was supported by the National Research Foundation of Korea (NRF) grant funded by the Korea government (MEST) (Grant No. NRF-2013R1A2A1A01016165 and No. 20120008283), and the IT R&D program of MKE/KEIT (Grant No. 10041416, the core technology development of light and space adaptable new mode display for energy saving on 7 inch and 2 W).

Supporting Information Available: Circuit diagram of 3 × 3 array of 2D planar micro-supercapacitor; photographs of 3 × 3 micro-supercapacitor array taken under strain from 0 to 30%; AFM images of spin-coated PI film; patterned deposition of SWCNTs. This material is available free of charge *via* the Internet at http://pubs.acs.org.

REFERENCES AND NOTES

1. Kim, D.-H.; Ahn, J.-H.; Choi, W.-M.; Kim, H.-S.; Kim, T.-H.; Song, J.; Huang, Y. Y.; Zhuangjian, L.; Chun, L.; Rogers, J. A. Stretchable and Foldable Silicon Integrated Circuits. *Science* **2008**, *320*, 507–511.
2. Kim, D.-H.; Song, J.; Choi, W. M.; Kim, H.-S.; Kim, R.-H.; Liu, Z.; Huang, Y. Y.; Hwang, K.-C.; Zhang, Y.; Rogers, J. A. Materials and Noncoplanar Mesh Designs for Integrated Circuits with Linear Elastic Responses to Extreme Mechanical Deformations. *Proc. Natl. Acad. Sci. U.S.A.* **2008**, *105*, 18675–18680.
3. Shin, G.; Bae, M. Y.; Lee, H. J.; Hong, S. K.; Yoon, C. H.; Zi, G.; Rogers, J. A.; Ha, J. S. SnO_2 Nanowire Logic Devices on Deformable Nonplanar Substrates. *ACS Nano* **2011**, *5*, 10009–10016.
4. Sekitani, T.; Nakajima, H.; Maeda, H.; Fukushima, T.; Aida, T.; Hata, K.; Someya, T. Stretchable Active-Matrix Organic Light-Emitting Diode Display Using Printable Elastic Conductors. *Nat. Mater.* **2009**, *8*, 494–499.
5. Hu, X.; Krull, P.; de Graff, B.; Dowling, K.; Rogers, J. A.; Arora, W. J. Stretchable Inorganic-Semiconductor Electronic Systems. *Adv. Mater.* **2011**, *23*, 2933–2936.
6. Park, S.-I.; Xiong, Y.; Kim, R.-H.; Elvikis, P.; Meitl, M.; Kim, D.-H.; Wu, J.; Yoon, J.; Yu, C.-J.; Liu, Z.; *et al.* Printed Assemblies of Inorganic Light-Emitting Diodes for Deformable and Semitransparent Displays. *Science* **2009**, *325*, 977–981.
7. Ko, H. C.; Stoykovich, M. P.; Song, J.; Malyarchuk, V.; Choi, W. M.; Yu, C.-J.; Geddes, J. B., III; Xiao, J.; Wang, S.; Huang, Y.; *et al.* A Hemispherical Electronic Eye Camera Based on Compressible Silicon Optoelectronics. *Nature* **2008**, *454*, 748–753.
8. Shin, G.; Jung, I.; Malyarchuk, V.; Song, J.; Wang, S.; Ko, H. C.; Huang, Y.; Ha, J. S.; Rogers, J. A. Micromechanics and Advanced Designs for Curved Photodetector Arrays in Hemispherical Electronic-Eye Cameras. *Small* **2010**, *6*, 851–856.
9. Jung, I.; Shin, G.; Malyarchuk, V.; Ha, J. S.; Rogers, J. A. Paraboloid Electronic Eye Cameras Using Deformable Arrays of Photodetectors in Hexagonal Mesh Layouts. *Appl. Phys. Lett.* **2010**, *96*, 021110.
10. Malyarchuk, V.; Jung, I.; Rogers, J. A.; Shin, G.; Ha, J. S. Experimental and Modeling Studies of Imaging with Curvilinear Electronic Eye Cameras. *Opt. Express* **2010**, *18*, 27346–27358.
11. Jung, I.; Xiao, J.; Malyarchuk, V.; Lub, C.; Li, M.; Liu, Z.; Yoon, J.; Huang, Y.; Rogers, J. A. Dynamically Tunable Hemispherical Electronic Eye Camera System with Adjustable Zoom Capability. *Proc. Natl. Acad. Sci. U.S.A.* **2011**, *108*, 1788–1793.
12. Kim, D.-H.; Kim, Y.-S.; Amsden, J.; Panilaitis, B.; Kaplan, D. L.; Omenetto, F. G.; Zakin, M. R.; Rogers, J. A. Silicon Electronics on Silk as a Path to Bioresorbable, Implantable Devices. *Appl. Phys. Lett.* **2009**, *95*, 133701.
13. Viventi, J.; Kim, D.-H.; Moss, J. D.; Kim, Y.-S.; Blanco, J. A.; Annetta, N.; Hicks, A.; Xiao, J.; Huang, Y.; Callans, D. J.; *et al.* A Conformal, Bio-Interfaced Class of Silicon Electronics for Mapping Cardiac Electrophysiology. *Sci. Transl. Med.* **2010**, *2*, 24ra22.
14. Kim, D.-H.; Viventi, J.; Amsden, J. J.; Xiao, J.; Vigeland, L.; Kim, Y.-S.; Blanco, J. A.; Panilaitis, B.; Frechette, E. S.; Contreras, D.; *et al.* Dissolvable Films of Silk Fibroin for Ultrathin, Conformal Bio-Integrated Electronics. *Nat. Mater.* **2010**, *9*, 511–517.
15. Kim, R.-H.; Kim, D.-H.; Xiao, J.; Kim, B. H.; Park, S.-I.; Panilaitis, B.; Ghaffari, R.; Yao, J.; Li, M.; Liu, Z.; *et al.* Waterproof AlInGaP Optoelectronics on Stretchable Substrates with Applications in Biomedicine and Robotics. *Nat. Mater.* **2010**, *9*, 929–937.
16. Kim, D.-H.; Lu, N.; Ghaffari, R.; Kim, Y.-S.; Lee, S. P.; Xu, L.; Wu, J.; Kim, R.-H.; Song, J.; Liu, Z.; *et al.* Materials for Multifunctional Balloon Catheters with Capabilities in Cardiac Electrophysiological Mapping and Ablation Therapy. *Nat. Mater.* **2011**, *10*, 316–323.
17. Lee, J.; Wu, J.; Shi, M.; Yoon, J.; Park, S.-I.; Li, M.; Liu, Z.; Huang, Y.; Rogers, J. A. Stretchable GaAs Photovoltaics with Designs That Enable High Areal Coverage. *Adv. Mater.* **2011**, *23*, 986–991.
18. Xu, S.; Zhang, Y.; Cho, J.; Lee, J.; Huang, X.; Jia, L.; Fan, J. A.; Su, Y.; Su, J.; Zhang, H.; *et al.* Stretchable Batteries with Self-Similar Serpentine Interconnections and Integrated Wireless Recharging Systems. *Nat. Commun.* **2013**, *4*, 1543.
19. Koo, M.; Park, K.-I.; Lee, S. H.; Suh, M.; Jeon, D. Y.; Choi, J. W.; Kang, K.; Lee, K. J. Bendable Inorganic Thin-Film Battery for Fully Flexible Electronic Systems. *Nano Lett.* **2012**, *12*, 4810–4816.
20. Gaikwad, A. M.; Zamarayeva, A. M.; Rousseau, J.; Chu, H.; Derin, I.; Steingart, D. A. Highly Stretchable Alkaline Batteries Based on an Embedded Conductive Fabric. *Adv. Mater.* **2012**, *24*, 5071–5076.
21. Lee, H.; Yoo, J.-K.; Park, J. H.; Kim, J. H.; Kang, K.; Jung, Y. S. A Stretchable Polymer−Carbon Nanotube Composite Electrode for Flexible Lithium-Ion Batteries: Porosity Engineering by Controlled Phase Separation. *Adv. Energy Mater.* **2012**, *2*, 976–982.

22. Ren, J.; Li, L.; Chen, C.; Chen, X.; Cai, Z.; Qiu, L.; Wang, Y.; Zhu, X.; Peng, H. Twisting Carbon Nanotube Fibers for Both Wire-Shaped Micro-Supercapacitor and Micro-Battery. *Adv. Mater.* **2013**, *25*, 1155–1159.
23. Li, X.; Gu, T.; Wei, B. Dynamic and Galvanic Stability of Stretchable Supercapacitors. *Nano Lett.* **2012**, *12*, 6366–6371.
24. Niu, Z.; Dong, H.; Zhu, B.; Li, J.; Hng, H. H.; Zhou, W.; Chen, X.; Xie, S. Highly Stretchable, Integrated Supercapacitors Based on Single-Walled Carbon Nanotube Films with Continuous Reticulate Architecture. *Adv. Mater.* **2013**, *25*, 1058–1064.
25. Kang, Y. J.; Chung, H.; Kim, W. 1.8-V Flexible Supercapacitors with Asymmetric Configuration Based on Manganese Oxide, Carbon Nanotubes, and a Gel Electrolyte. *Synth. Met.* **2013**, *166*, 40–44.
26. Kang, Y. J.; Chun, S.-J.; Lee, S.-S.; Kim, B.-Y.; Kim, J. H.; Chung, H.; Lee, S.-Y.; Kim, W. All-Solid-State Flexible Supercapacitors Fabricated with Bacterial Nanocellulose Papers, Carbon Nanotubes, and Triblock-Copolymer Ion Gels. *ACS Nano* **2012**, *6*, 6400–6406.
27. Xiao, X.; Li, T.; Yang, P.; Gao, Y.; Jin, H.; Ni, W.; Zhan, W.; Zhang, X.; Cao, Y.; Zhong, J.; *et al.* Fiber-Based All-Solid-State Flexible Supercapacitors for Self-Powered Systems. *ACS Nano* **2012**, *6*, 9200–9206.
28. Yu, C.; Masarapu, C.; Rong, J.; Wei, B.; Jiang, H. Stretchable Supercapacitors Based on Buckled Single-Walled Carbon Nanotube Macrofilms. *Adv. Mater.* **2009**, *21*, 4793–4797.
29. El-Kady, M. F.; Kaner, R. B. Scalable Fabrication of High-Power Graphene Micro-Supercapacitors for Flexible and On-Chip Energy Storage. *Nat. Commun.* **2013**, *4*, 1475.
30. Wang, X.; Liu, B.; Wang, Q.; Song, W.; Hou, X.; Chen, D.; Cheng, Y.-b.; Shen, G. Three-Dimensional Hierarchical $GeSe_2$ Nanostructures for High Performance Flexible All-Solid-State Supercapacitors. *Adv. Mater.* **2013**, *25*, 1479–1486.
31. Kim, D.-H.; Xiao, J.; Song, J.; Huang, Y.; Rogers, J. A. Stretchable, Curvilinear Electronics Based on Inorganic Materials. *Adv. Mater.* **2010**, *22*, 2108–2124.
32. Lodge, T. P. A Unique Platform for Materials Design. *Science* **2008**, *321*, 50–51.
33. Zhang, S.; Lee, K. H.; Frisbie, C. D.; Lodge, T. P. Ionic Conductivity, Capacitance, and Viscoelastic Properties of Block Copolymer-Based Ion Gels. *Macromolecules* **2011**, *44*, 940–949.
34. Lee, J.; Kaake, L. G.; Cho, J. H.; Zhu, X.-Y.; Lodge, T. P.; Frisbie, C. D. Ion Gel-Gated Polymer Thin-Film Transistors: Operating Mechanism and Characterization of Gate Dielectric Capacitance, Switching Speed, and Stability. *J. Phys. Chem. C* **2009**, *113*, 8972–8981.
35. Armand, M.; Endres, F.; MacFarlane, D. R.; Ohno, H.; Scrosati, B. Ionic-Liquid Materials for the Electrochemical Challenges of the Future. *Nat. Mater.* **2009**, *8*, 621–629.
36. Ohno, H. *Electrochemical Aspects of Ionic Liquids*; Wiley & Sons, Inc.: Hoboken, NJ, 2005.
37. Kim, B.; Chung, H.; Kim, W. High-Performance Supercapacitors Based on Vertically Aligned Carbon Nanotubes and Nonaqueous Electrolytes. *Nanotechnology* **2012**, *23*, 155401.
38. Porte, A. R.; Liem, S. Y.; Popelier, P. L. A. Room Temperature Ionic Liquids Containing Low Water Concentrations—A Molecular Dynamics Study Phys. *Chem. Chem. Phys.* **2008**, *10*, 4240–4248.
39. Metz, S. J.; van de Ven, W. J. C.; Potreck, J.; Mulder, M. H. V.; Wessling, M. Transport of Water Vapor and Inert Gas Mixtures through Highly Selective and Highly Permeable Polymer Membranes. *J. Membr. Sci.* **2005**, *251*, 29–41.
40. Shin, G.; Yoon, C. H.; Bae, M. Y.; Kim, Y. C.; Hong, S. K.; Rogers, J. A.; Ha, J. S. Stretchable Field-Effect-Transistor Array of Suspended SnO_2 Nanowires. *Small* **2011**, *7*, 1181–1185.